AGU100 ADVANCING EARTH AND SPACE SCIENCE

Geophysical Research Letters

RESEARCH LETTER

10.1029/2018GL079740

Key Points:
- Relationship between shallow slow slip events and seismicity is reported at the southernmost Ryukyu Trench for the first time
- Spatiotemporal seismicity does not adequately correlate with propagation of slow slip but is dominated by mainshock-aftershock sequences
- High-pressure fluid activity likely has a key role in the initiation of episodic slow slip events and subsequent seismicity

Supporting Information:
- Supporting Information S1
- Figure S1
- Figure S2
- Figure S3
- Figure S4

Correspondence to:
S. K. Chen,
sean80254@gmail.com

Citation:
Chen, S. K., Wu, Y.-M., & Chan, Y.-C. (2018). Episodic slow slip events and overlying plate seismicity at the southernmost Ryukyu Trench. *Geophysical Research Letters*, *45*, 10,369–10,377. https://doi.org/10.1029/2018GL079740

Received 27 JUL 2018
Accepted 24 SEP 2018
Accepted article online 1 OCT 2018
Published online 10 OCT 2018

Episodic Slow Slip Events and Overlying Plate Seismicity at the Southernmost Ryukyu Trench

Sean Kuanhsiang Chen[1,2], Yih-Min Wu[1,2,3], and Yu-Chang Chan[1]

[1]Academia Sinica, Institute of Earth Sciences, Taipei, Taiwan, [2]Department of Geosciences, National Taiwan University, Taipei, Taiwan, [3]NTU Research Center for Future Earth, National Taiwan University, Taipei, Taiwan

Abstract Shallow slow slip events accompanied by seismicity has been increasingly reported in subduction zones during the last decade; however, the relationship between shallow slip events and seismicity is unclear. We report episodic slow slip events and seismicity at the southernmost Ryukyu Trench. The inversion results from GPS-derived cumulative displacements indicate that the slow slip events occur offshore in northeastern Taiwan on the shallow subduction interface, where high seismic V_P/V_S ratios applies. Seismicity is observed above the subduction interface for locations of significant variations in the V_P/V_S ratio and does not follow the migration of peak slip along the subduction interface. We calculated the temporal evolution between the seismicity and the propagation of slow slip events and determined that seismicity is not primarily driven by slip propagation. The spatiotemporal relationship, coupled with the V_P/V_S ratio, suggests that high-pressure fluid activity may be crucial to episodes of slow slip events and seismicity.

Plain Language Summary Slow slip events are a member of the slow-earthquake family observed by geodetic measurements in global subduction zones in the past 15 years. Shallow slow slip events are considered to be important for the megathrust earthquake cycle of the shallowest locked zone. Recently, shallow slow slip events accompanied by different seismic behaviors has been increasingly reported. This paper reports episodic, shallow slow slip events accompanied by overlying plate seismicity at the southernmost Ryukyu Trench and analyzes their relationship. We discover that the spatiotemporal relationship between the propagation of slow slip and seismicity is weak, which infers that they may not have a causal relationship. We suggest that the initiation of shallow slow slip events and subsequent seismicity was probably caused by high-pressure fluid activity. The interpretation may reveal the cause of many shallow slow slip events as a broad phenomenon.

1. Introduction

Slow slip events (SSEs), with slow rupture velocities and long durations from days, months, to years, is regarded as an aseismic mechanism that releases accumulated stress on subduction interfaces. The mechanism primarily occurs in deep regions of subduction interfaces under the seismogenic zone (e.g., Dragert et al., 2001; Schwartz & Rokosky, 2007). Recently, SSEs are increasingly occurring in shallow regions of subduction interfaces over the seismogenic zone or near trenches (e.g., Araki et al., 2017; Wallace et al., 2016). Activity of shallow SSEs is considered to be a key effect on the megathrust earthquake cycle of the shallowest subduction interface (Obara & Kato, 2016; Saffer & Wallace, 2015). Shallow SSEs may be accompanied by seismicity, tremors, or very low-frequency earthquakes that locate near the source region of shallow SSEs. Seismicity was predominantly observed in several subductions at shallow depths (<30 km), for example, Hikurangi, Japan Trench, and Ecuador (Delahaye et al., 2009; Ito et al., 2013; Vallée et al., 2013). Along the Hikurangi subduction interface and Ecuador subduction interfaces, seismicity that accompanies shallow SSEs occurred near depths of <30 and <15 km, respectively, at the downdip of the shallow SSE region (Delahaye et al., 2009; Vallée et al., 2013). However, the relationship between shallow SSEs and seismicity remains unclear. Recently, biannual SSEs in the southern Ryukyu Trench (Heki & Kataoka, 2008) were observed to be modulated by earthquake swarms from the Okinawa Trough (Tu & Heki, 2017). A modulation is an acceleration of southward movement after recurrence of earthquake swarms in a decadal time scale. In this study, we focus on the southernmost Ryukyu Trench, where seismic activity is high and may be modulated by seasonal horizontal motion detected by a continuous GPS (cGPS) network in the eastern Taiwan (Chen et al., 2014).

The Ryukyu Trench is considered to be a Mariana-type subduction (Uyeda & Kanamori, 1979) based on the main driving force of active back-arc rifting (Sibuet et al., 1987). Seventeen-year geodetic observations

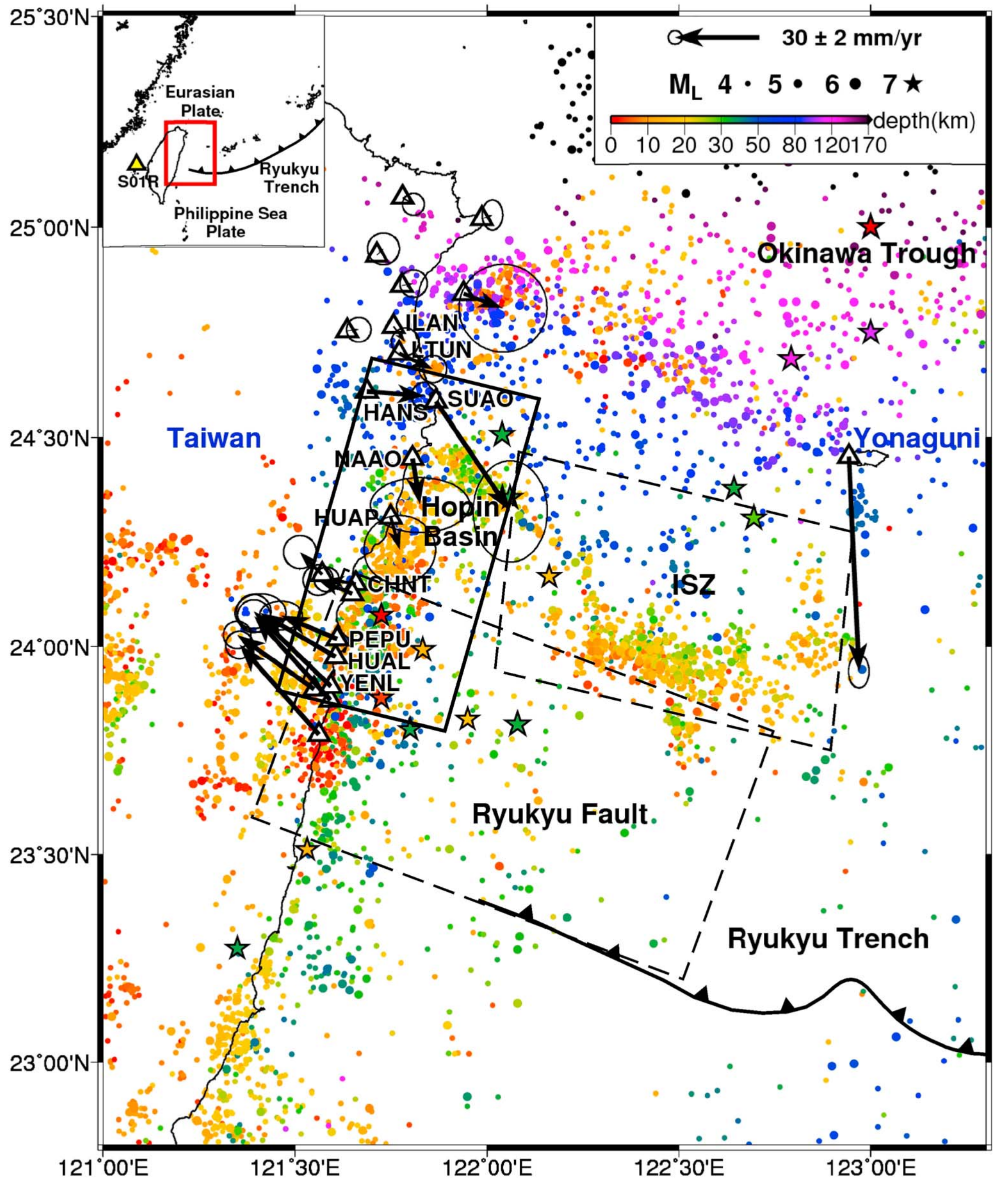

Figure 1. Tectonics, surface motion, and seismicity of the southernmost Ryukyu Trench. The dashed rectangles show the Ryukyu Fault, which is a locked region of the trench proposed by Hsu et al. (2012) and the interplate seismogenic zone (ISZ; Kao, 1998; Theunissen et al., 2010). The trench axis is modified from Theunissen et al. (2010) and Hsu et al. (2012). The black arrows represent the continuous GPS (cGPS) horizontal velocities at each station in the white triangle with respect to the S01R station in the yellow triangle with 95% confidence ellipses from GLOBK. The colored dots are relocated earthquakes at depths from 1991 to 2016, which is updated from Wu, Chang, et al. (2008), and the stars show historical $M \geq 7.0$ earthquakes (Theunissen et al., 2010). The box region includes clear transient displacements from named cGPS stations and is used to calculate seismicity.

indicate that SSEs frequently occurred along the Ryukyu Trench at the shallow depths (Nishimura, 2014). However, the observations did not include the southernmost segment, which is the only segment that lacks evidence of SSEs. The southernmost Ryukyu Trench rapidly converges at a rate of 12.5 cm/year (Hsu et al., 2012), which produces high seismic activity in the subduction zone (Figure 1). The maximum historical earthquake size in the last 300 years is ~M_w 7.7 and limited to the range M_w 7.0–7.5 (Theunissen et al., 2010). The limitation of earthquake size seems to conflict with an expectation of one maximum size when an ~60-Ma young oceanic plate converges with rapid velocity (Ando et al., 2009). Thus, an aseismic mechanism was suggested to exist in the interplate seismogenic zone (ISZ) (Kao, 1998; Figure 1) for the release of seismic moment budgets. This suggestion is supported by an estimation of weak seismic coupling on the ISZ (Theunissen et al., 2010), which implies that an aseismic slip has a major role on a fault slip in multiple earthquake cycles. Here we present new evidence of surface transient displacements in northeastern Taiwan to directly verify the slow slip behavior. We identified a correlation between cGPS transient displacements and seismicity in the surrounding areas, which provides an excellent opportunity to examine the relationship between SSEs and seismicity in the southernmost Ryukyu Trench.

2. Data and Methods

2.1. cGPS, Earthquake Data, and Processing

cGPS observations are derived from the edge of the southernmost Ryukyu Trench, including 21 cGPS stations in northeastern Taiwan and 1 GNSS station on Yonaguni Island (Figure 1). The cGPS data information, processing, and analysis of the position time series from January 2004 to June 2017 were described in Text S1 in the supporting information S1. The analysis attempted to highlight transient signals on raw position time series and used a criterion to systematically identify transient displacements (refer to Text S1). In the analysis, when transient displacements are detected by many cGPS stations in northeastern Taiwan, they are not detected at the GNSS station on Yonaguni Island. To examine velocity changes in the position time series after high seismic activity as observed at the southern Ryukyu Trench (Tu & Heki, 2017), a 1-year secular velocity before onset times and after stop times of each transient displacement was calculated to estimate the degree of velocity change.

Since tremor/very low-frequency earthquake data are lacking in our study area (Chao et al., 2012; Nakamura & Sunagawa, 2015), seismicity data are used to examine whether seismic activity spatiotemporally correlates to cGPS-derived transient displacements. A relocated earthquake catalog in the Taiwan region from 1991 to 2016 updated from Wu, Chang, et al. (2008) was employed by selecting events in the vicinity of the cGPS transient displacements in a box region (Figure 1), with local magnitudes (M_L) of $\geq$2.0 and depths of $\leq$30 km. The criterion in the space is consistent with observations of seismicity that accompany SSEs from subduction zones (e.g., Delahaye et al., 2009; Vallée et al., 2013); that is, seismicity tends to occur at shallow depths of subduction zones beneath surface transient displacements. If the temporal seismicity is correlated with the period between the onset/stop times of cGPS transient displacements, the transients will be recognized as SSEs. Other aspects of temporal seismicity that are not correlated with any transient displacement will not be discussed. The temporal seismicity was calculated for monthly and 6-day activity to perform a comparison with different timescales in position time series (Figure 2). In the analysis, transient displacements can correspond to regional seismicity using our assumption and criterion, and we did not identify distinct transient displacements without seismicity in the 13-year cGPS observations. To explore the temporal relationship between temporal seismicity and transient displacements, the cumulative number of earthquakes was calculated with the cumulative displacements of the peak displacement during each SSE. To examine whether earthquake swarms have a role in transient displacements, an approach of spatiotemporal double-link declustering (Wu & Chiao, 2006) was applied to remove aftershock sequences in the box region, which is dominated by $M_L \geq 5.0$ events (Figure S2).

2.2. cGPS Time Series Inversion

To understand a first-order feature of spatiotemporal evolution of SSEs, three-component transient displacements are inverted using a time-dependent nonlinear TDefnode code (McCaffrey, 2009) for the slip distribution on a subduction interface. TDefnode inverts first-order features of a position time series and can search a coherence of transient displacements from each station (e.g., Koulali et al., 2017; Wallace et al., 2017). At the southernmost Ryukyu Trench, the ISZ can be aseismic (Kao, 1998; Theunissen et al., 2010) but the location is distant from the cGPS transient displacements detected in northeastern Taiwan (Figure 1) and is too close to Yonaguni Island, where transient displacements are undetected. Here we searched a single fault model along the subduction interface for each SSE (refer to Text S2 in supporting information S1) and then estimated the slip distribution by dividing the calculated fault model into uniform grids. The grid size with a resolution of 10 km $\times$ 10 km is established on the fault planes to perform TDefnode for spatiotemporal distributions of slip (McCaffrey, 2009; refer to Text S3 in supporting information S1). To estimate the migration rate and azimuth of the SSEs by the approach of McCaffrey (2009), onset times of slip are delayed at each cGPS station if required. Cumulative moments during each SSE were estimated by a magnitude dependence on fault parameters in the Taiwan region (Yen & Ma, 2011).

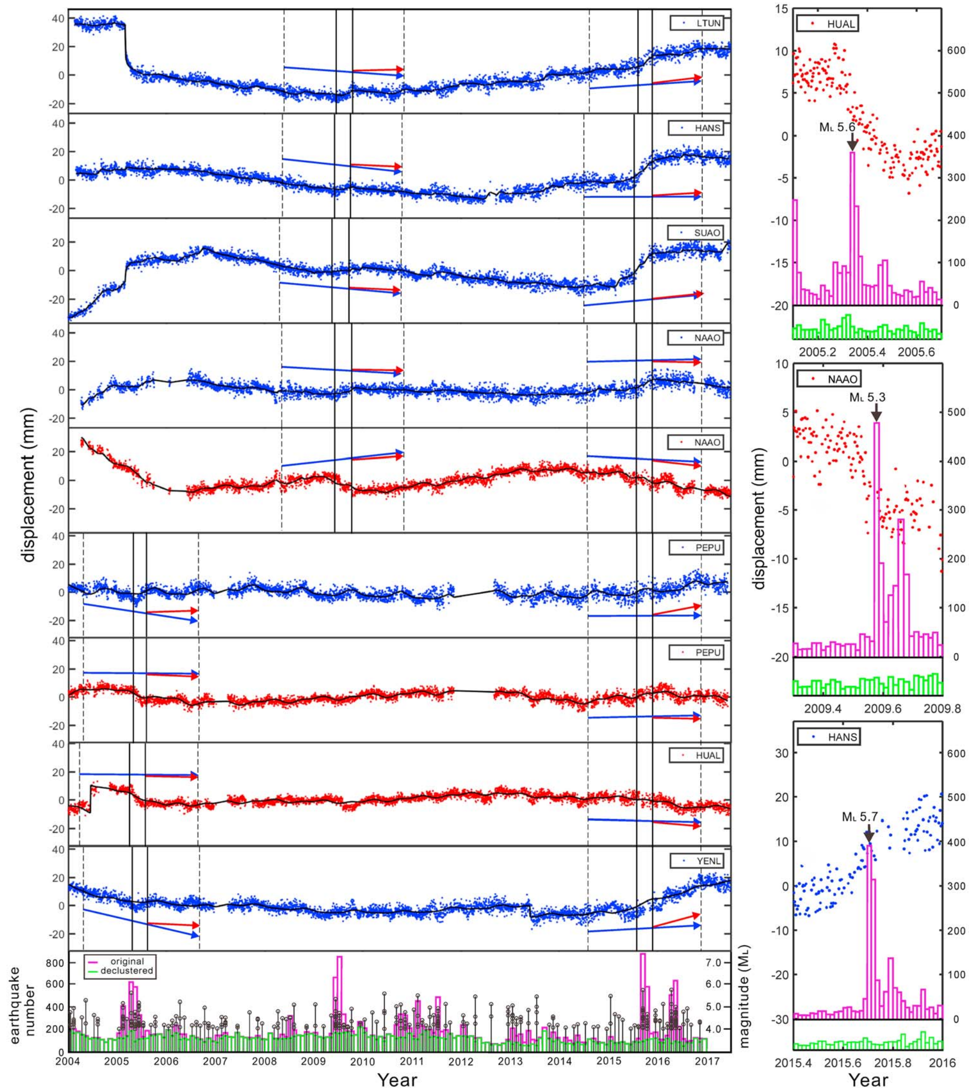

Figure 2. Position time series at the northeastern Taiwan and temporal seismicity from a box region of Figure 1. The blue time series and red time series denote the east component and north component, respectively, and the inner black curves are model predictions. The black solid lines show the onset/stop times of slip at each station, and the dashed lines are 1 year before the onset/stop and 1 year after the onset/stop, respectively. The blue arrows and red arrows represent 1-year secular velocities before the onset/stop and 1-year secular velocities after the onset/stop, respectively. The number of earthquakes with $M_L \geq 2.0$ and depths of $\leq$30 km and the events with $M_L \geq 4.0$ are shown in the bar charts and open circles, respectively. The subfigures on the right show approximately a half-year period, which covers the onset/stop times of slip in each slow slip event at the named station.

3. Shallow SSEs, Seismicity, and Spatiotemporal Evolution of Slip

Figure 2 shows episodic SSEs, including durations from 2 to 4 months on cGPS horizontal components in northeastern Taiwan. Figure 3 shows the cumulative horizontal displacements during each SSE and the locations of the most active seismicity during the SSEs. The episodic SSEs occurred April to June 2005, June to October 2009, and August to November 2015. The 2005 SSE triggered surface cumulative displacements southeastward to a peak of 10 mm in the vicinity of the PEPU and HUAL stations (Figure 3). The 2009 and 2015 SSEs triggered southeastward displacements and eastward displacements to a peak of 10 and 12 mm, respectively, in the vicinity of the LTUN, SUAO, and NAAO stations (Figure 3). During the SSEs, declustered seismicity did not show significant activity in the cGPS transient displacements (Figure 2), which indicates that earthquake swarms may not participate in the process of SSEs. However, raw seismicity

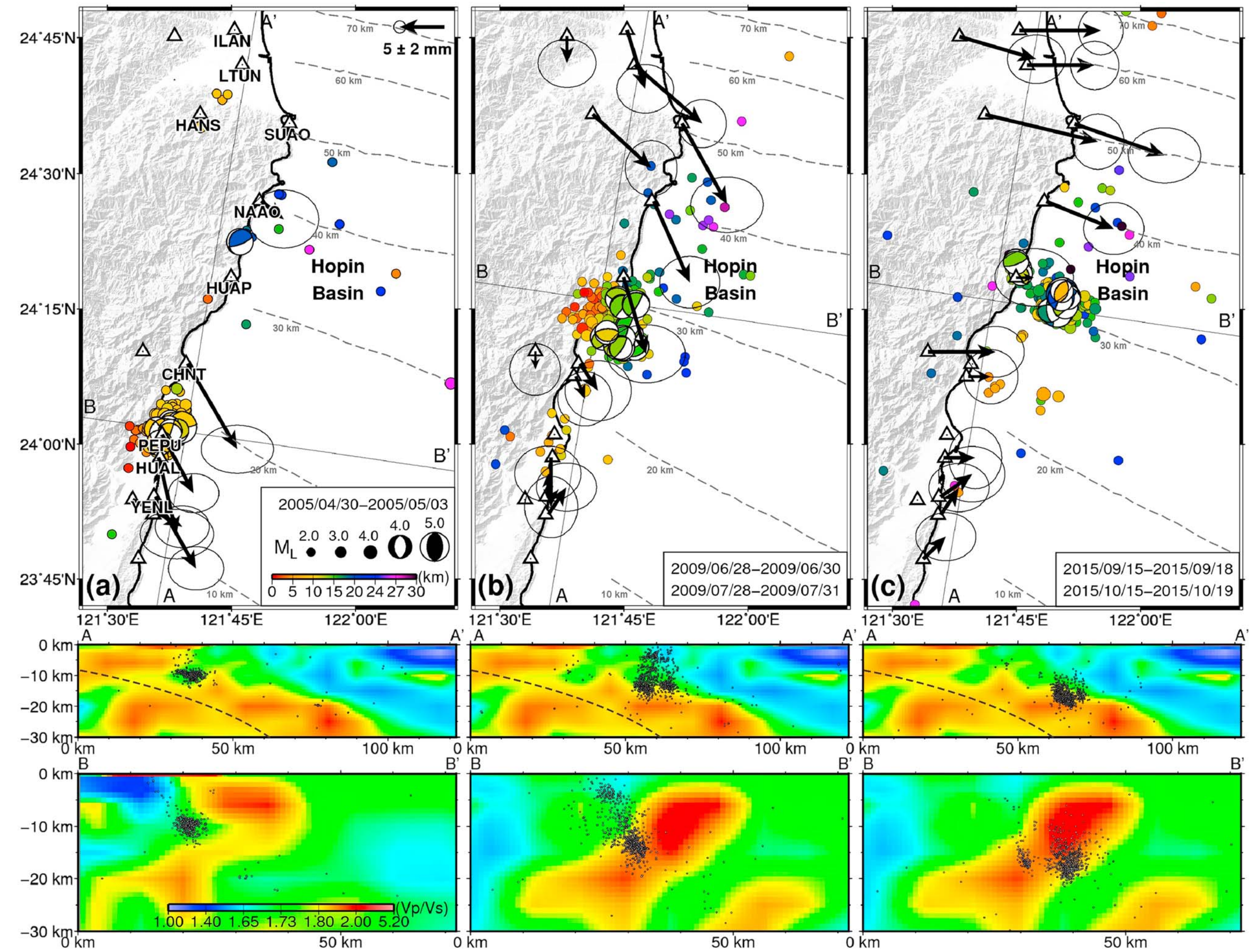

Figure 3. Locations with most active seismicity and cumulative horizontal displacements at the southernmost Ryukyu Trench during slow slip events. The vertical cumulative displacements were a few millimeters at some of the continuous GPS stations and are disregarded. The periods of most active seismicity are shown in each top figure. The colored circles ($2.0 \le M_L \le 4.0$) and beach balls ($M_L \ge 4.0$) represent earthquakes at depths of ≤30 km derived from a relocated catalog (Wu, Chang, et al., 2008) and a *P* wave first motion focal mechanism catalog (Wu, Zhao, et al., 2008), respectively. The dashed curves represent the subduction interface (Wu et al., 2009). The seismic V_P/V_S ratios at depths along the profiles are derived from Huang et al. (2014).

indicates significant activity in the transient displacements, which is substantially higher than that of other periods (Figure 2). For the 2005 SSE, seismicity occurred in the initial durations of the SSE dominated by a M_L 5.6 mainshock-aftershock sequence (Figure 2), which is located beneath the region of surface peak displacement (Figure 3). During the early to middle duration of the 2009 SSE and the 2015 SSE, both of seismicity rapidly increased and were dominated by two mainshock-aftershock sequences located near the region of surface peak displacement (Figure 3), with the largest events of M_L 5.3 and M_L 5.7, respectively. Time periods of the mainshock-aftershock sequences are shown in Figure 3; they represent the most active seismicity in each SSE. The spatial seismicity approximately distributed above the shallow subduction interface, which ranges from depths of 1 to 20 km (Figure 3). The overlying plate seismicity, with location uncertainties of ~1 to 3 km in horizontal and ~4 km in depth (e.g., Wu et al., 2013), is relatively localized, which differs from the majority of previous observations: seismicity that accompanies SSEs occurred on or near the subduction interface. During each SSE, the epicenters of the overlying plate seismicity spatially correlate with the areas of surface cumulative displacements (Figure 3), which implies that the SSE source is likely located near the locations of seismicity and surface displacements. An examination of the focal mechanisms of $M_L \ge 4.0$ earthquakes suggests that the seismicity related faulting styles to thrust faulting or a mixture of strike-slip faulting and thrust faulting (Figure 3). This finding is consistent with regional stress regimes in the region of Figure 3, which is dominated by a high $A\phi$ value

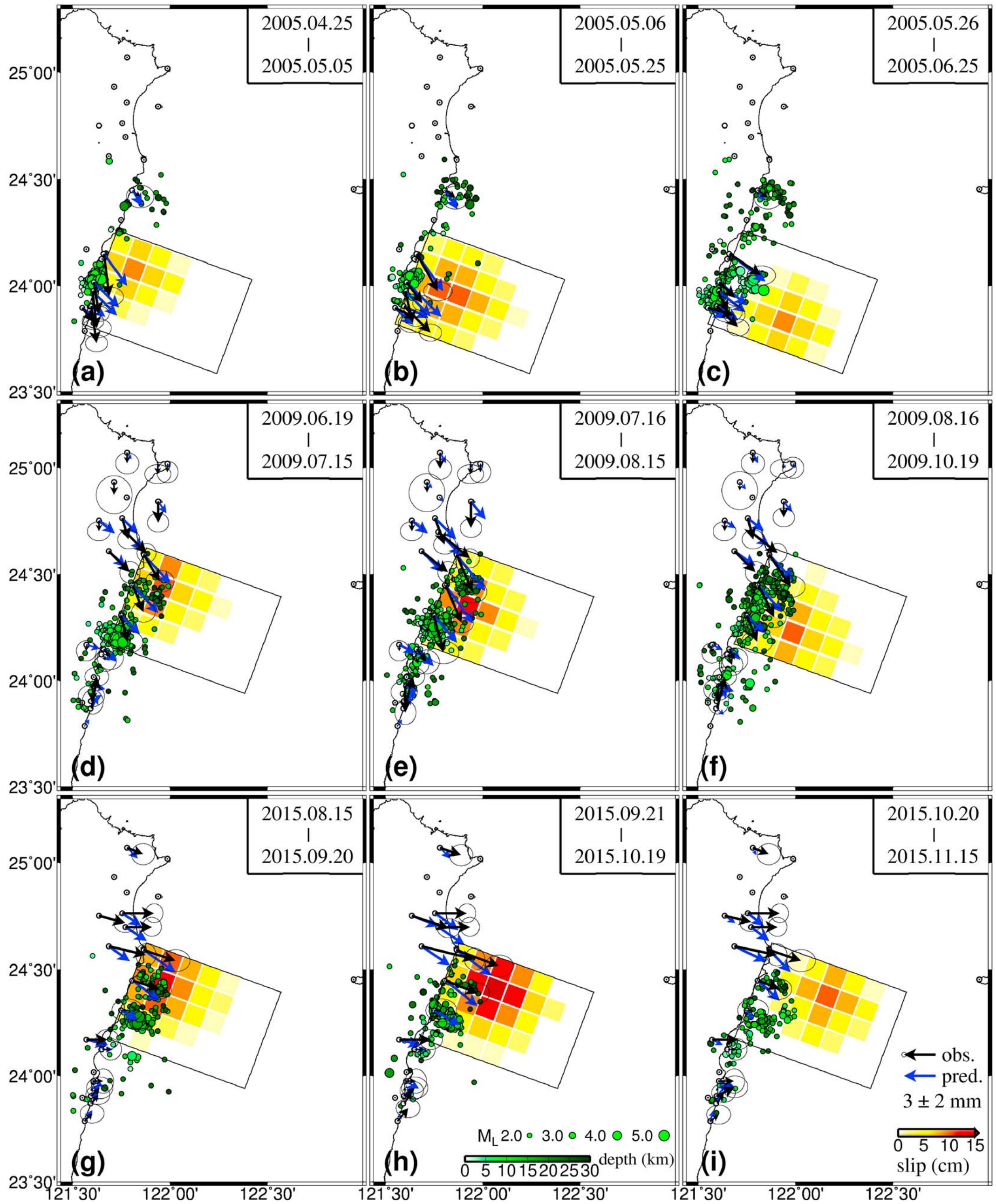

Figure 4. Spatiotemporal evolution of each slow slip event (SSE) and seismicity. Subfigures (a–c), (d–f), and (g–i) represent SSEs in 2005, 2009, and 2015, respectively. The color bar shows the slip amounts on the best-fitting fault models. The black arrows and blue arrows represent the horizontal displacements for the continuous GPS stations from observations and model predictions, respectively. The green circles in the box region of Figure 1 represent the earthquakes with $M_L \geq 2.0$ at depths of ≤30 km for each time slice.

domain at depths of ≤20 km (Chen et al., 2017) as a thrust faulting regime (refer to the definition of $A\phi$ in Text S4 in supporting information S1). In addition, a possible remaining slip was detected after episodic SSEs (Figure 2) in northeastern Taiwan; however, it is quantitatively minor compared with the slip of SSEs (refer to Text S5 in supporting information S1 and Figure S3).

In Figure 4, spatiotemporal evolution of slip is shown on the best-fitting fault model. The fault models for three SSEs with a given length of 70 km suggest that they dip northward at 15° with an orientation of N20° and a width of 50 km and approximately cover the depth range of the subduction interface from 10 to 40 km. For the 2005 SSE, the aseismic slip occurred south of the two subsequent SSEs at shallower depths. Spatiotemporal evolution of slip on the fault shows a southeastward migration at an average speed of 0.35 km/day and a peak slip of ~10 cm near the fault plane center (Figure 4). For the 2009 and 2015 SSEs, the inversion results indicate that they shared the same fault plane but performed different spatiotemporal evolution of slip. The 2009 SSE migrated toward the southeast at a slower average speed of 0.3 km/day and attained a peak slip of 12 cm on the west of the fault plane center (Figure 4). The 2015 SSE migrated to the east at a faster average speed of 0.4 km/day and attained an ~15-cm peak slip near the downdip region of the fault plane (Figure 4). The predictions of slip by the best-fitting fault models adequately fit first-order transient displacements at most of the cGPS stations within the observational uncertainties.

The maximum cumulative moments during the 2005, 2009, and 2015 SSEs are estimated to approximately equal earthquake failure of M_w 6.4, M_w 6.5, and M_w 6.6, respectively. The estimation is similar to the cumulative moments that are released from SSEs in the neighboring southern Ryukyu Trench, which was estimated to be an average of M_w 6.6 (Heki & Kataoka, 2008). Considering seismicity and the potential remaining slip, the maximum cumulative moments and the moments of the 2005 SSE, 2009 SSE, and 2015 SSE are M_w 6.5, M_w 6.7, and M_w 6.8, respectively. The quantifications reveal that episodic shallow SSEs can reduce a portion of accumulated stress on the shallow portion of the southernmost Ryukyu subduction zone. In addition, we noticed that the overlying plate seismicity did not follow the migrations of the peak slip (Figure 4). Shallow SSEs and concurrent seismicity are not spatially well correlated in a few subduction zones as in Boso, Japan (Ozawa et al., 2007) and Hikurangi, New Zealand (Delahaye et al., 2009; Wallace et al., 2017). This phenomenon may reveal that the spatial relationship between the seismicity and propagation of shallow SSE is weak, which implies other physical mechanisms.

4. Discussion

4.1. Possible Mechanism of Shallow SSEs and Seismicity

Recently, geophysical surveys, drilling, and laboratory experiments from the shallowest trenches in Nankai, Japan and Hikurangi, New Zealand indicate that shallow SSEs occur in the fault zones with overpressured fluid, low effective stress, and frictional transition (Araki et al., 2017; Saffer & Wallace, 2015; Wallace et al., 2016). An examination of the offshore seismic velocities of northeastern Taiwan from the tomography results (Huang et al., 2014; Wu et al., 2009) indicates that the shallow subduction interface and SSE faults are covered by high V_P/V_S ratios with low V_S values that are located in the vicinity of Hoping Basin (Figure 3). The high V_P/V_S ratios imply a fluid-rich environment that is consistent with the concept of shallow SSEs occurrence in regions of overpressured fluid (Saffer & Wallace, 2015), which is recently observed near the SSE fault in the neighboring southern Ryukyu Trench (Yamamoto et al., 2018). The high V_P/V_S ratios elongated vertically near the significant variation in the V_P/V_S ratios, where the overlying plate seismicity occurred (Figure 3). The location uncertainties of the seismicity are within the range of the significant variation in the V_P/V_S ratios. The feature may reveal that high-pressure fluid ascends from the subduction interface to shallow depths, which causes the overlying plate seismicity. We infer that when the Philippine Sea Plate subducts, the dehydration causes the fluid to migrate along the subduction interface and vertically within the overlying plate, which triggers episodic SSEs and seismicity, respectively. The inference shows agreement with a recent seismic observation and concept of fluid-triggered SSEs and seismicity from Kanto, Japan (Nakajima & Uchida, 2018).

4.2. Temporal Relationship Between Shallow SSEs and Seismicity

In Figure S4, the cumulative number of earthquakes as a function of the cumulative peak displacements during each SSE is shown. A second-order polynomial relationship with varying dependence indicates that the number of earthquakes increased at a faster rate and a slower rate than displacements in the early periods of SSEs and later periods of SSEs, respectively. The temporal relationship is similar to previous observations in the Hikurangi (Delahaye et al., 2009) and Ecuador subduction interfaces (Vallée et al., 2013). However, only small-magnitude seismicity ($M_w \leq 4.1$) was identified in the studies. In this study, the temporal seismicity during each SSE was dominated by aftershock sequences from $M_L \geq 5.3$ earthquakes (Figure 2). If the temporal seismicity is driven by propagation of aseismic slip, a linear relationship between the cumulative displacements and the cumulative number of earthquakes is expected, as observed between the afterslip and the aftershock after occurrences of large earthquakes (e.g., Hsu et al., 2006). Considering the temporal relationship between declustered seismicity and SSEs, a linear relationship is also nonexistent because the seismicity did not increase with the activity of each SSE and are similar before, within, and after the durations (Figure 2). The temporal evidence, coupled with the spatial separation of seismicity and aseismic slip (Figures 3 and 4), causes us to infer that seismicity is not primarily driven by the propagation of SSEs. Recently, an environment of high $A\phi$ values and low b-values was reported in the region of overlying plate seismicity (Wu et al., 2018). The environment may imply that larger earthquakes can dominate over smaller earthquakes in a state of high differential stress. High-pressure fluid activity may necessitate an increase in pore-fluid pressure and the triggering of $M_L > 5.0$ mainshock-aftershock sequences in this region.

4.3. Role of Shallow SSEs in Megathrust Earthquake

In the shallowest locked zone of the southernmost Ryukyu Trench, the magnitude of a potential megathrust earthquake was estimated to be $M_w \geq 8.0$ based on neotectonic architecture (Shyu et al., 2005) and $7.5 \leq M_w \leq 8.7$ based on geodetic measurements (Hsu et al., 2012). The estimations may need to be rethought because of the finding of shallow SSEs. Kao (1998) and Theunissen et al. (2010) inferred that aseismic slip can exist in the ISZ at depths from 15 to 35 km. Our results indicate that the SSE fault is located further west of the ISZ at a similar depth range and may cover the western half of ISZ. The difference reveals that the slip did not simultaneously occur on the ISZ, at least the eastern half, when the SSE fault moved during the data period of 2004 to 2017. The feature may imply that aseismic slip is not restricted within a single fault zone and can laterally vary along the subduction interface. The lateral variation of SSE behavior is significant from our study area to the neighboring southern Ryukyu Trench, as reported that SSEs in that Trench are biannually repeated at a deeper depth range of 20–45 km (Tu & Heki, 2017). This finding may imply a spatiotemporal heterogeneity in the interplate coupling along the strike of the total southern Ryukyu Trench, which is crucial for further understanding of earthquake cycles along the Trench. If the episodic SSEs repeat in all timescales instead of only during our 13-year data periods, this finding will help us explain a phenomenon at the southernmost Ryukyu Trench: For a rapid convergence rate of 12.5 cm/year (Hsu et al., 2012), the maximum earthquake sizes are restricted with magnitudes of M_w 7.7 in the last 300 years (Theunissen et al., 2010). Further observations and modeling would better explain the lateral variation of aseismic slip, interplate coupling, and earthquake cycles along the southernmost Ryukyu Trench.

5. Conclusions

This paper identified episodic SSEs and the source region at the southernmost Ryukyu Trench for the first time. The source region of SSEs is estimated to locate at a low-angle fault on the shallow subduction interface, which is covered by a region of high seismic V_P/V_S ratios. The shallow SSEs with durations from 2 to 4 months in 2005, 2009, and 2015 are accompanied by overlying plate seismicity with maximum magnitudes of M_L 5.6, M_L 5.3, and M_L 5.7, respectively. The seismicity occurred above the SSE fault in locations where the V_P/V_S ratios significantly vary and does not spatially correlate well with the propagation of SSEs. The seismicity and propagation of SSEs are also not well temporally correlated. High-pressure fluid activity revealed by high V_P/V_S ratios can be a key mechanism of the initiation of episodic SSEs and subsequent seismicity.

Acknowledgments
We thank Ya-Ju Hsu for the helpful discussion. We also thank the Editor Lucy Flesch, the reviewer Junichi Nakajima, and another anonymous reviewer for their constructive comments while improving the manuscript. This research is supported by the Ministry of Science and Technology (MOST) in Taiwan (MOST 106-2116-M-002-019-MY3) and The Featured Areas Research Center Program within the framework of the Higher Education Sprout Project by the Ministry of Education (MOE) in Taiwan. The cGPS data used in this study are available at http://gps.earth.sinica.edu.tw/. The relocated earthquake and focal mechanism catalogs used in this study can be obtained from http://seismology.gl.ntu.edu.tw/download.htm.

References

Ando, M., Nakamura, M., Matsumoto, T., Furukawa, M., Tadokoro, K., & Furumoto, M. (2009). Is the Ryukyu subduction zone in Japan coupled or decoupled? The necessity of seafloor crustal deformation observation. *Earth, Planets and Space*, *61*(9), 1031–1039. https://doi.org/10.1186/BF03352954

Araki, E., Saffer, D. M., Kopf, A. J., Wallace, L. M., Kimura, T., Machida, Y., et al., & IODP Expedition 365 shipboard scientists (2017). Recurring and triggered slow-slip events near the trench at the Nankai trough subduction megathrust. *Science*, *356*(6343), 1157–1160. https://doi.org/10.1126/science.aan3120

Chao, K., Peng, Z., Wu, C., Tang, C. C., & Lin, C. H. (2012). Remote triggering of non-volcanic tremor around Taiwan. *Geophysical Journal International*, *188*(1), 301–324. https://doi.org/10.1111/j.1365-246X.2011.05261.x

Chen, S. K., Chan, Y. C., Hu, J. C., & Kuo, L. C. (2014). Current crustal deformation at the junction of collision to subduction around the Hualien area, Taiwan. *Tectonophysics*, *617*, 58–78. https://doi.org/10.1016/j.tecto.2014.01.014

Chen, S. K., Wu, Y. M., Hsu, Y. J., & Chan, Y. C. (2017). Current crustal deformation of the Taiwan orogen reassessed by cGPS strain-rate estimation and focal mechanism stress inversion. *Geophysical Journal International*, *210*(1), 228–239. https://doi.org/10.1093/gji/ggx165

Delahaye, E. J., Townend, J., Reyners, M. E., & Rogers, G. (2009). Microseismicity but no tremor accompanying slow slip in the Hikurangi subduction zone, New Zealand. *Earth and Planetary Science Letters*, *277*(1-2), 21–28. https://doi.org/10.1016/j.epsl.2008.09.038

Dragert, H., Wang, K., & James, T. S. (2001). A silent slip event on the deeper Cascadia subduction interface. *Science*, *292*(5521), 1525–1528. https://doi.org/10.1126/science.1060152

Heki, K., & Kataoka, T. (2008). On the biannually repeating slow-slip events at the Ryukyu trench, southwestern Japan. *Journal of Geophysical Research*, *113*, B11402. https://doi.org/10.1029/2008JB005739

Hsu, Y. J., Ando, M., Yu, S. B., & Simons, M. (2012). The potential for a great earthquake along the southernmost Ryukyu subduction zone. *Geophysical Research Letters*, *39*, L14302. https://doi.org/10.1029/2012GL052764

Hsu, Y. J., Simons, M., Avouac, J. P., Galetzka, J., Sieh, K., Chlieh, M., et al. (2006). Frictional afterslip following the 2005 Nias-Simeulue earthquake, Sumatra. *Science*, *312*(5782), 1921–1926. https://doi.org/10.1126/science.1126960

Huang, H. H., Wu, Y. M., Song, X. D., Chang, C. H., Lee, S. C., Chang, T. M., & Hsieh, H. H. (2014). Joint V_P and V_S tomography of Taiwan: Implications for subduction-collision orogeny. *Earth and Planetary Science Letters*, *392*, 177–191. https://doi.org/10.1016/j.epsl.2014.02.026

Ito, Y., Hino, R., Kido, M., Fujimoto, H., Osada, Y., Inazu, D., et al. (2013). Episodic slow slip events in the Japan subduction zone before the 2011 Tohoku-Oki earthquake. *Tectonophysics*, *600*, 14–26. https://doi.org/10.1016/j.tecto.2012.08.022

Kao, H. (1998). Can great earthquakes occur in the southernmost Ryukyu arc-Taiwan region? *Terrestrial, Atmospheric and Oceanic Sciences Journal*, *9*(3), 487–508. https://doi.org/10.3319/TAO.1998.9.3.487(TAICRUST)

Koulali, A., McClusky, S., Wallace, L., Allgeyer, S., Tregoning, P., D'Anastasio, E., & Benavente, R. (2017). Slow slip events and the 2016 Te Araroa M_w 7.1 earthquake interaction: Northern Hikurangi subduction, New Zealand. *Geophysical Research Letters*, *44*, 8336–8344. https://doi.org/10.1002/2017GL074776

McCaffrey, R. (2009). Time-dependent inversion of three-component continuous GPS for steady and transient sources in northern Cascadia. *Geophysical Research Letters*, *36*, L07304. https://doi.org/10.1029/2008GL036784

Nakajima, J., & Uchida, N. (2018). Repeated drainage from megathrust during episodic slow slip. *Nature Geoscience*, *11*(5), 351–356. https://doi.org/10.1038/s41561-018-0090-z

Nakamura, M., & Sunagawa, N. (2015). Activation of very low frequency earthquakes by slow slip events in the Ryukyu Trench. *Geophysical Research Letters*, *42*, 1076–1082. https://doi.org/10.1002/2014GL062929

Nishimura, T. (2014). Short-term slow slip events along the Ryukyu Trench, southwestern Japan, observed by continuous GNSS. *Earth, Planets and Space*, *1*(1), 22. https://doi.org/10.1186/s40645-014-0022-5

Obara, K., & Kato, A. (2016). Connecting slow earthquakes to huge earthquakes. *Science*, *353*(6296), 253–257. https://doi.org/10.1126/science.aaf1512

Ozawa, S., Suito, H., & Tobita, M. (2007). Occurrence of quasi-periodic slow slip off the east coast of the Boso peninsula, central Japan. *Earth, Planets and Space*, *59*(12), 1241–1245. https://doi.org/10.1186/BF03352072

Saffer, D. M., & Wallace, L. M. (2015). The frictional, hydrologic, metamorphic and thermal habitat of shallow slow earthquakes. *Nature Geoscience*, *8*(8), 594–600. https://doi.org/10.1038/ngeo2490

Schwartz, S. Y., & Rokosky, J. M. (2007). Slow slip events and seismic tremor at circum-Pacific subduction zones. *Reviews of Geophysics*, *45*, RG3004. https://doi.org/10.1029/2006RG000208

Shyu, J. B. H., Sieh, K., Chen, Y. G., & Liu, C. S. (2005). Neotectonic architecture of Taiwan and its implications for future large earthquakes. *Journal of Geophysical Research*, *110*, B08402. https://doi.org/10.1029/2004JB003251

Sibuet, J. C., Letouzey, J., Barbier, F., Charvet, J., Foucher, J. P., Hilde, T. W. C., et al. (1987). Back arc extension in the Okinawa trough. *Journal of Geophysical Research*, *92*, 14,041–14,063. https://doi.org/10.1029/JB092iB13p14041

Theunissen, T., Font, Y., Lallemand, S., & Liang, W. T. (2010). The largest instrumentally recorded earthquake in Taiwan: Revised location and magnitude, and tectonic significance of the 1920 event. *Geophysical Journal International*, *183*(3), 1119–1133. https://doi.org/10.1111/j.1365-246X.2010.04813.x

Tu, Y., & Heki, K. (2017). Decadal modulation of repeating slow slip event activity in the southwestern Ryukyu Arc possibly driven by rifting episodes at the Okinawa Trough. *Geophysical Research Letters*, *44*, 9308–9313. https://doi.org/10.1002/2017GL074455

Uyeda, S., & Kanamori, H. (1979). Back-arc opening and the mode of subduction. *Journal of Geophysical Research*, *84*, 1049–1061. https://doi.org/10.1029/JB084iB03p01049

Vallée, M., Nocquet, J. M., Battaglia, J., Font, Y., Segovia, M., Régnier, M., et al. (2013). Intense interface seismicity triggered by a shallow slow slip event in the Central Ecuador subduction zone. *Journal of Geophysical Research: Solid Earth*, *118*, 2965–2981. https://doi.org/10.1002/jgrb.50216

Wallace, L. M., Kaneko, Y., Hreinsdóttir, S., Hamling, I., Peng, Z., Bartlow, N., et al. (2017). Large-scale dynamic triggering of shallow slow slip enhanced by overlying sedimentary wedge. *Nature Geoscience*, *10*(10), 765–770. https://doi.org/10.1038/ngeo3021

Wallace, L. M., Webb, S. C., Ito, Y., Mochizuki, K., Hino, R., Henrys, S., et al. (2016). Slow slip near the trench at the Hikurangi subduction zone, New Zealand. *Science*, *352*(6286), 701–704. https://doi.org/10.1126/science.aaf2349

Wu, Y. M., Chang, C. H., Kuo-Chen, H., Huang, H. H., & Wang, C. Y. (2013). On the use of explosion records for examining earthquake location uncertainty in Taiwan. *Terrestrial, Atmospheric and Oceanic Sciences*, *24*(4-2), 685–694. https://doi.org/10.3319/TAO.2013.01.31.01(T)

Wu, Y. M., Chang, C. H., Zhao, L., Teng, T. L., & Nakamura, M. (2008). A comprehensive relocation of earthquakes in Taiwan from 1991 to 2005. *Bulletin of the Seismological Society of America*, *98*(3), 1471–1481. https://doi.org/10.1785/0120070166

Wu, Y. M., Chen, S. K., Huang, T. C., Huang, H. H., Chao, W. A., & Koulakov, I. (2018). Relationship between earthquake *b*-values and crustal stresses in a young orogenic belt. *Geophysical Research Letters*, *45*, 1832–1837. https://doi.org/10.1002/2017GL076694

Wu, Y. M., & Chiao, L. Y. (2006). Seismic quiescence before the 1999 Chi-Chi, Taiwan M_w 7.6 earthquake. *Bulletin of the Seismological Society of America*, *96*(1), 321–327. https://doi.org/10.1785/0120050069

Wu, Y. M., Shyu, J. B. H., Chang, C. H., Zhao, L., Nakamura, M., & Hsu, S. K. (2009). Improved seismic tomography offshore northeastern Taiwan: Implications for subduction and collision processes between Taiwan and the southernmost Ryukyu. *Geophysical Journal International*, *178*(2), 1042–1054. https://doi.org/10.1111/j.1365-246X.2009.04180.x

Wu, Y. M., Zhao, L., Chang, C. H., & Hsu, Y. J. (2008). Focal mechanism determination in Taiwan by genetic algorithm. *Bulletin of the Seismological Society of America*, *98*(2), 651–661. https://doi.org/10.1785/0120070115

Yamamoto, Y., Takahashi, T., Ishihara, Y., Kaiho, Y., Arai, R., Obana, K., et al. (2018). Modeling the geometry of plate boundary and seismic structure in the southern Ryukyu Trench subduction zone, Japan, using amphibious seismic observations. *Journal of Geophysical Research: Solid Earth*, *123*, 1793–1809. https://doi.org/10.1002/2017JB015330

Yen, Y. T., & Ma, K. F. (2011). Source-scaling relationship for *M* 4.6–8.9 earthquakes, specifically for earthquakes in the collision zone of Taiwan. *Bulletin of the Seismological Society of America*, *101*(2), 464–481. https://doi.org/10.1785/0120100046